

---

# Uncertainty Quantification using Generative Approach

---

Yunsheng Zhang  
yunshzhang@gmail.com

## Abstract

We present the Incremental Generative Monte Carlo (IGMC) method, designed to measure uncertainty in deep neural networks using deep generative approaches. IGMC iteratively trains generative models, adding their output to the dataset, to compute the posterior distribution of the expectation of a random variable. We provide a theoretical guarantee of the convergence rate of IGMC relative to the sample size and sampling depth. Due to its compatibility with deep generative approaches, IGMC is adaptable to both neural network classification and regression tasks. We empirically study the behavior of IGMC on the MNIST digit classification task.

## 1 Introduction

Deep learning has found applications across many domains in recent years and has consistently achieved remarkable results (LeCun et al., 2015). While deep neural networks excel in predictive accuracy across various tasks, their predictions are not devoid of errors. *Uncertainty* can be defined as a measure of the divergence between predicted values and their ground-truth values. Quantifying the uncertainty in deep neural network prediction is crucial in several research fields. For example, in tasks requiring high-risk decision-making or stringent safety standards, such as medical image analysis (Nair et al., 2020; Roy et al., 2019; Seeböck et al., 2019) and autonomous vehicle control (Feng et al., 2018; Choi et al., 2019), uncertainty quantification can assist AI systems in assessing challenging situations. In reinforcement learning, uncertainty quantification can aid agents in improving their exploration strategies (Azizzadenesheli et al., 2018; Bellemare et al., 2016). Uncertainty quantification is also widely used in active learning (Gal et al., 2017; Shelmanov et al., 2021), explainable AI (Seuß, 2021), and few-shot learning (Zhang et al., 2021; Mukherjee and Awadallah, 2020).

There are many possible sources of uncertainty in neural network prediction, including data uncertainty, model uncertainty (Hüllermeier and Waegeman, 2021), or out-of-distribution (OOD) of test data (Lee et al., 2017; Hendrycks and Gimpel, 2016). Traditional deep learning methods cannot capture uncertainty. Various methods have been proposed to quantify uncertainty, such as a single deterministic network to predict uncertainty (Oberdiek et al., 2018; Ju et al., 2022; Sensoy et al., 2018). Augment the input data at test-time (Wang et al., 2019; Ayhan and Berens, 2018). The Bayesian method (Gal and Ghahramani, 2015; Blundell et al., 2015). The ensemble method trains several models and combines their prediction to estimate uncertainty during inference (Valdenegro-Toro, 2019; Lakshminarayanan et al., 2017).

This paper focuses on the uncertainty of models that predict a random variable’s expectation or conditional expectation. Note that classification (which provides probabilities for each class label as continuous values) and regression can be described as forms of conditional expectation learning. Given a set of independent and identically distributed (i.i.d.) samples  $S$  from a random variable  $X$ , our method, named *Incremental Generative Monte Carlo* (IGMC), determines the posterior cumulative distribution function (CDF) for  $\mu = E[X]$ , thereby quantifying the uncertainty. Unlike Bayesian methods, our method’s definition of the posterior CDF is not based on likelihoods or parameter priors but rather on a generative approach. A *generative approach* is a rule or algorithm that converts any sample set into a generative model. The models and learning algorithms of variational autoencoder (Kingma and Welling, 2022) and generative adversarial network (Goodfellow et al., 2014) can be considered examples of generative approaches.

Compared to other methods, our method requires fewer modifications to the model and its learning algorithm. Notably, a classification model can naturally function as a generative model, obviating the need for changes when addressing classification tasks, which implies that the classification algorithm has the inherent ability to gauge classification uncertainty. We theoretically and empirically show the distance between the posterior CDF produced by IGMC and the ground-truth posterior CDF. Lastly, we empirically study IGMC’s behavior on the MNIST digit classification task (Deng, 2012), using a convolutional neural network as the classification model.

## 2 Preliminary

Let  $X$  denote a random variable with the support  $[0, 1]$ , with an unknown expectation value  $\mu = E[X]$ . We draw  $M$  independent samples from  $X$ , symbolized as  $x_1, x_2, \dots, x_M$ , and the empirical estimate for  $\mu$  is given by  $\hat{\mu} = \frac{x_1 + x_2 + \dots + x_M}{M}$ .

One way to define uncertainty is by assessing the probability that  $\mu$  and  $\hat{\mu}$  deviate by a certain amount  $t$ . We can determine the upper limit of this uncertainty through Hoeffding’s inequality:

$$\Pr(|\hat{\mu} - \mu| \geq t) \leq 2 \exp(-2Mt^2) \quad (1)$$

This inequality illustrates that the uncertainty shrinks exponentially as the sample size increases. Another commonly used Bayesian method interprets  $\mu$  as a posterior distribution conditioned on  $x_1, x_2, \dots, x_M$ . With a known form of parameter  $\theta$ , and its prior  $\Pr(\theta)$  and likelihoods  $\Pr(x|\theta)$ , the Bayesian posterior probability is given as follow:

$$\Pr(\theta|x_1, \dots, x_M) = \frac{\Pr(x_1, \dots, x_M|\theta)}{\int \Pr(x_1, \dots, x_M|\theta') \cdot \Pr(\theta')d\theta'} \cdot \Pr(\theta) \quad (2)$$

Thus, the posterior probability of  $\mu$  can be obtained by:

$$\Pr(\mu|x_1, \dots, x_M) = \int \Pr(\mu|\theta)\Pr(\theta|x_1, \dots, x_M)d\theta \quad (3)$$

The uncertainty can be measured by the dispersion of posterior distribution, such as the standard deviation of  $\Pr(\mu|x_1, \dots, x_M)$ .

## 3 Generative approach as uncertainty quantifier

In this section, we present a method for quantifying uncertainty using generative approaches. We first give the definition of the generative approach. The generative approach, denoted as  $\Phi$ , can transform any samples drawn from  $X$  into a generative model. The generative model represents a random variable with a support range identical to  $X$ . Note that we will focus only on one-dimensional  $X$  in this section.

Consider a Bernoulli trial as an illustration. For any  $M$  observations represented by  $x_1, \dots, x_M$ , let  $a$  denote the number of success events among them. Then  $\Phi(x_1, \dots, x_M) := \text{Bern}(a/M)$  is a well-defined generative approach. For notational simplicity, we assume  $\Phi$  is deterministic, and our results can generalize to the case that  $\Phi$  is nondeterministic.

### 3.1 Definition of Incremental Generative Distribution Function

The intuition behind using a generative approach to compute the posterior distribution of  $E[X]$  is as follows: as the sample size of  $X$  grows, the uncertainty of  $E[X]$  will decrease. Suppose we have a good generative approach  $\Phi$  that can effectively describe the relationship between observations and distributions. In that case, we can generate enough samples by utilizing the generative approach  $\Phi$  to represent the posterior distribution in a simple and computable form.

Using mathematical notation, considering calculation of the posterior CDF  $\Pr(\mu < t|\mathcal{S})$  of  $\mu$ , we use  $\mathcal{S}$  to represent  $x_1, \dots, x_M$  for short. We can expand the function by applying the total probability formula:

---

**Algorithm 1** Incremental Generative Monte Carlo

---

```
1: Given generative approach  $\Phi$ ; i.i.d. samples  $\{x_1, \dots, x_M\}$  from  $X$ ; sample size  $N$ ; sampling depth  $H$ .
2: for  $n = 1, \dots, N$  do
3:   Initialize the dataset  $\mathcal{S}_n \leftarrow \{x_1, \dots, x_M\}$ 
4:   for  $h = 1, \dots, H$  do
5:     get generative model  $\gamma \leftarrow \Phi(\mathcal{S}_n)$ 
6:     sample  $y_h \sim \gamma$ 
7:     add  $y_h$  into  $\mathcal{S}_n$ 
8:   end for
9:   set  $\mu_n \leftarrow \frac{\sum x_i + \sum y_h}{M+H}$ 
10: end for
11: set  $\hat{F}_{H,N}^\Phi(t|\mathcal{S}) \leftarrow \sum_{n=1}^N \mathbb{I}(\mu_n \leq t)$ 
12: Return  $\hat{F}_{H,N}^\Phi(\cdot|\mathcal{S})$ 
```

---

$$\Pr(\mu < t|\mathcal{S}) = \int_0^1 dy_1 \Pr(y_1|\mathcal{S}) \Pr(\mu < t|\mathcal{S}, y_1) \quad (4)$$

Here  $\Pr(y_1|\mathcal{S})$  is the probability density function of  $\Phi(\mathcal{S})$ . We can then proceed to apply the full probability formula to  $\Pr(\mu < t|\mathcal{S}, y_1)$ :

$$\Pr(\mu < t|\mathcal{S}, y_1) = \int_0^1 dy_2 \Pr(y_2|\mathcal{S}, y_1) \Pr(\mu < t|\mathcal{S}, y_1, y_2) \quad (5)$$

Here  $\Pr(y_2|\mathcal{S}, y_1)$  is the probability density function of  $\Phi(\mathcal{S}, y_1)$ . Repeating this process for  $H$  times, we define:

$$F_H^\Phi(t|\mathcal{S}) = \underbrace{\int_0^1 dy_1 \Pr(y_1|\mathcal{S}) \cdots \int_0^1 dy_H \Pr(y_H|\mathcal{S}, y_1, \dots, y_{H-1}) \mathbb{I}\left(\frac{\sum x + \sum y}{M+H} < t\right)}_{\text{applying law of total probability for } H \text{ times}} \quad (6)$$

We substituted the posterior probability with an indicator function in the last item. Since  $\Pr(\mu < t|\mathcal{S}, y_1, \dots, y_H)$  approaches  $\mathbb{I}(\frac{\sum x + \sum y}{M+H} < t)$  arbitrarily close as  $H \rightarrow \infty$ , we define

$$F_\infty^\Phi(t|\mathcal{S}) = \lim_{H \rightarrow \infty} F_H^\Phi(t|\mathcal{S}) \quad (7)$$

Then  $F_\infty^\Phi(t|\mathcal{S})$  should correspond to the posterior CDF of  $E[X]$  that we aim to obtain. In the above formulation, only the generative approach  $\Phi$  needs to be provided. Therefore, Eq. (6) and (7) can serve as the definition for the posterior CDF based on the specified generative approach  $\Phi$ . We term  $F_\infty^\Phi(t|\mathcal{S})$  as the *Incremental Generative Distribution Function* (IGDF).

From the Bayesian perspective, the definition of posterior probability requires the prior and the likelihood. Interestingly, our method does not require parameters prior explicitly. Notably, this absence is not contradictory because  $\Phi$  already has the information about the parameter prior and likelihood inherently. This claim is supported by the fact that  $F_\infty^\Phi(t|\mathcal{S})$  matches the posterior distribution from the Bayesian method when  $\Phi(\mathcal{S})$  consistently follows the Bayesian posterior predictive distribution for any sample set  $\mathcal{S}$ .

### 3.2 Incremental Generative Monte Carlo

In Section 3.1, we define the IGDF  $F_\infty^\Phi(t|\mathcal{S})$  based on the generative approach  $\Phi$ . Intuitively, for a large  $H$ ,  $F_H^\Phi(t|\mathcal{S})$  is an approximation of  $F_\infty^\Phi(t|\mathcal{S})$ . However, obtaining the closed form of either  $F_\infty^\Phi(t|\mathcal{S})$  or  $F_H^\Phi(t|\mathcal{S})$  may not always be possible for a given  $\Phi$ . Since each  $y_h$  in Eq. (6) can be

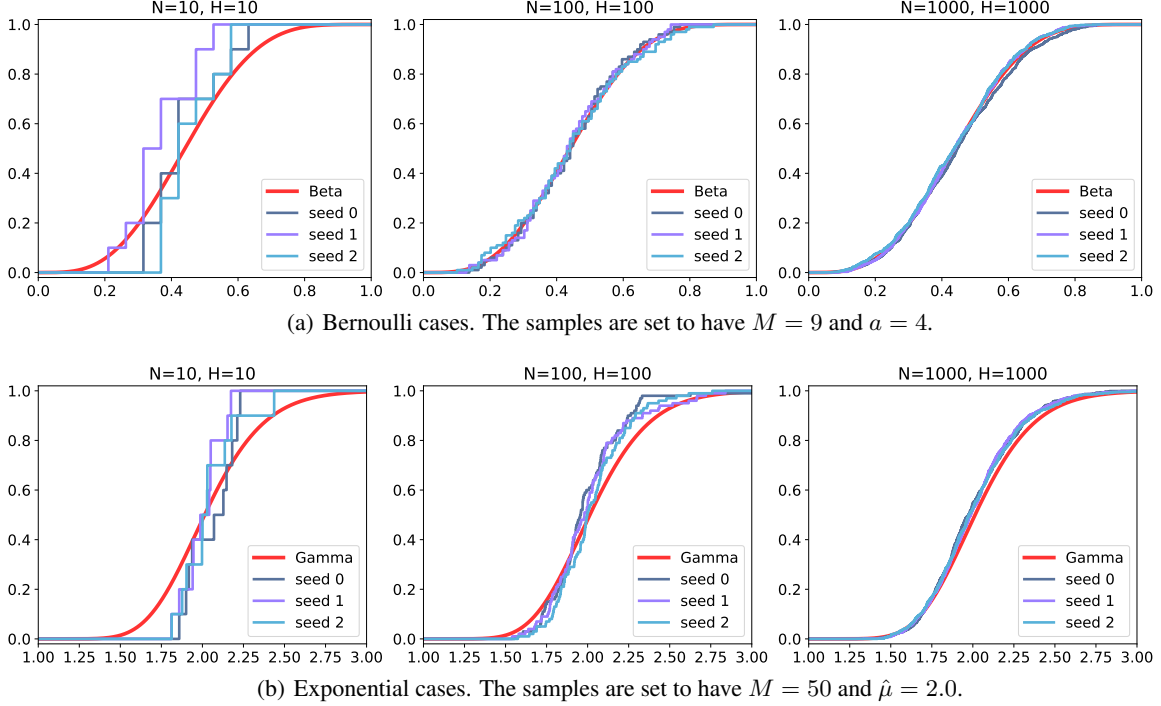


Figure 1: Experimental curves of IGMC for specific  $N$  and  $H$  values.

sampled from  $\Phi(\mathcal{S}, y_1, \dots, y_{h-1})$ , we can approximate  $F_H^\Phi(t|\mathcal{S})$  using the Monte Carlo method. We present the complete algorithm, which we call *Incremental Generative Monte Carlo* (IGMC), in Algorithm 1. The  $\hat{F}_{H,N}^\Phi(\cdot|\mathcal{S})$  returned by IGMC is the Monte Carlo estimation of  $F_H^\Phi(\cdot|\mathcal{S})$  with a sample size of  $N$ .

We empirically test IGMC for situations where  $X$  follows Bernoulli and exponential distribution. For the cases where  $X$  follows the Bernoulli distribution, we set  $\Phi(x_1, \dots, x_M) := \text{Bern}(a/M)$ , where  $a$  is the number of success events. For the cases that  $X$  follows the exponential distribution, we set  $\Phi(x_1, \dots, x_M) := \text{Exponential}(1/\hat{\mu})$ , with  $\hat{\mu}$  being the average of  $x_1, \dots, x_M$ . All experiments run with three different random seeds. The configurations are  $N = 10, H = 10$ ; and  $N = 100, H = 100$ ; and  $N = 1000, H = 1000$ . Additionally, we plotted the posterior distribution of  $\mu$  by the Bayesian method for reference, that is,  $\text{Beta}(a, M - a)$  and  $\text{Gamma}(M, M\hat{\mu})$ . The resulting curves of  $\hat{F}_{H,N}^\Phi$  are shown in Fig. 1(a) and Fig. 1(b).

The figure indicates that when  $N$  and  $H$  are greater than a hundred, the  $\hat{F}_{H,N}^\Phi$  produced by IGMC aligns closely with the distribution derived from the Bayesian method. When  $X$  follows the Bernoulli distribution, the Bayesian posterior predictive distribution follows  $\text{Bern}(a, M - a)$ . Thus, as  $N$  and  $H$  increase, the  $\hat{F}_{H,N}^\Phi$  will converge to  $\text{Beta}(a, M - a)$ . However, when  $X$  follows an exponential distribution, the  $\hat{F}_{H,N}^\Phi$  does not match the Gamma distribution, even as  $N$  and  $H$  approach infinity. This discrepancy is because the Bayesian posterior predicts a Lomax distribution instead of  $\text{Exp}(1/\hat{\mu})$  in this situation.

In addition to empirical evaluations, it is crucial to verify the convergence of  $\hat{F}_{H,N}^\Phi$  to the IGDF  $F_\infty^\Phi$  and determine its rate of convergence. The following theorem provides a theoretical guarantee under some conditions.

**Theorem 1.** *If support of  $X$  is  $[0, 1]$ , and  $\Phi$  satisfies  $\mathbb{E}[\Phi(x_1, \dots, x_M)] = \sum_{i=1}^M x_i/M$  for  $\forall M \in \mathbb{N}^+$  and  $\forall x_1, \dots, x_M \in [0, 1]^M$ . Then the expectation of  $L^1$  distance between  $F_\infty^\Phi$  and  $\hat{F}_{H,N}^\Phi$  is  $O(\sqrt{\frac{1}{N}} + \sqrt{\frac{1}{H}})$ , where  $\hat{F}_{H,N}^\Phi$  is the posterior CDF returned by IGMC (Algorithm 1) with sampling depth  $H$  and sample size  $N$ .*

---

**Algorithm 2** Deep Incremental Generative Monte Carlo for Classification Tasks

---

```
1: Given deep classification learning algorithm  $\Phi$ ; Training dataset  $\mathcal{D}$ ; sample size  $N$ ; sampling
   depth  $H$ ; Number of categories  $K$ ; Input  $x$  for classification and uncertainty quantification.
2: for  $n = 1, \dots, N$  do
3:   Initialize the dataset  $\mathcal{D}_n \leftarrow \mathcal{D}$ 
4:   for  $h = 1, \dots, H$  do
5:     initialize neural network parameters  $\theta$ 
6:     train  $\theta$  on dataset  $\mathcal{D}_n$  by  $\Phi$  until converge.
7:     compute  $\mathbf{p} \leftarrow f_\theta(x)$ 
8:     sample a label  $y_h \sim \mathbf{p}$ 
9:     add input-label pair  $(x, y_h)$  into  $\mathcal{D}_n$ 
10:  end for
11:  for  $k = 1, \dots, K$  do
12:    set  $\mu_{n,k} \leftarrow \sum_{h=1}^H \mathbb{I}(y_h = k)/H$ 
13:  end for
14: end for
15: for  $k = 1, \dots, K$  do
16:   set  $\hat{F}_{H,N}^\Phi(t, k|\mathcal{D}) \leftarrow \sum_{n=1}^N \mathbb{I}(\mu_{n,k} \leq t)$ 
17: end for
18: Return  $\hat{F}_{H,N}^\Phi(\cdot, \cdot|\mathcal{D})$ 
```

---

**Proof:** See Appendix A.

## 4 Deep Incremental Generative Monte Carlo

In this section, we extend Algorithm 1 to quantify the uncertainty in the predictions of deep neural networks. This is achieved by substituting  $\Phi$  with deep generative methods such as VAE (Kingma and Welling, 2022), GAN (Goodfellow et al., 2014), and Diffusion (Ho et al., 2020). For a discrete target space, a feed-forward neural network with a softmax activation function in the final layer can serve as  $\Phi$ . Different from Section 3, the deep neural network generally requires an input  $x$ . Thus, we must add  $(x, y_h)$  pair to the dataset  $\mathcal{D}_n$  rather than only  $y_h$ .

We take the classification task with  $K$  categories as an example. The pseudo-code is shown in Algorithm 2. Note in line 7,  $f_\theta(x)$  denotes the neural network’s output given input  $x$  and parameter  $\theta$ .  $\mathbf{p}$  is a  $K$ -dimensional vector where  $\mathbf{p}_k$  represents the probability that  $x$  belongs to class  $k$ . Let  $P_k$  be a random variable signifying the probability of input  $x$  belonging to class  $k$ . The outcome  $\hat{F}_{H,N}^\Phi(t, k|\mathcal{D})$  of Alg 2 represents the estimated posterior probability of  $P_k \leq t$ .

We evaluate Algorithm 2 on the MNIST digit classification task (Deng, 2012). The experimental model is a two-layer convolution neural network with 16 channels and ReLU activation functions, ending with a linear softmax classification layer. The initial dataset is the MNIST training dataset.

Labels										
0	100.0[0.00]	0.0[0.00]	0.0[0.00]	0.0[0.00]	0.0[0.00]	0.0[0.00]	0.0[0.00]	0.0[0.00]	0.0[0.00]	0.0[0.00]
1	0.0[0.00]	100.0[0.00]	0.0[0.00]	0.0[0.00]	0.0[0.00]	0.0[0.00]	0.0[0.00]	0.1[0.00]	0.0[0.00]	0.0[0.00]
2	0.0[0.00]	0.0[0.00]	100.0[0.00]	0.0[0.00]	0.0[0.00]	0.0[0.00]	0.0[0.00]	30.1[0.46]	0.0[0.00]	0.0[0.00]
3	0.0[0.00]	0.0[0.00]	0.0[0.00]	100.0[0.00]	0.0[0.00]	0.0[0.00]	0.0[0.00]	6.7[0.13]	0.0[0.00]	8.8[0.13]
4	0.0[0.00]	0.0[0.00]	0.0[0.00]	0.0[0.00]	84.2[0.28]	0.0[0.00]	0.0[0.00]	0.1[0.00]	0.0[0.00]	0.0[0.00]
5	0.0[0.00]	0.0[0.00]	0.0[0.00]	0.0[0.00]	0.0[0.00]	100.0[0.00]	0.0[0.00]	0.0[0.00]	0.0[0.00]	3.5[0.08]
6	0.0[0.00]	0.0[0.00]	0.0[0.00]	0.0[0.00]	0.0[0.00]	0.0[0.00]	100.0[0.00]	0.0[0.00]	0.0[0.00]	0.0[0.00]
7	0.0[0.00]	0.0[0.00]	0.0[0.00]	0.0[0.00]	2.4[0.03]	0.0[0.00]	0.0[0.00]	62.0[0.54]	0.0[0.00]	0.0[0.00]
8	0.0[0.00]	0.0[0.00]	0.0[0.00]	0.0[0.00]	0.0[0.00]	0.0[0.00]	0.0[0.00]	0.7[0.00]	100.0[0.00]	2.0[0.04]
9	0.0[0.00]	0.0[0.00]	0.0[0.00]	0.0[0.00]	13.2[0.23]	0.0[0.00]	0.0[0.00]	0.4[0.00]	0.0[0.00]	85.7[0.24]

Table 1: Results for images from MNIST test dataset.

The models are trained by the SGD optimizer with cosine learning rate decay. The learning rate is initiated to 0.002, and the momentum is set to 0.9. Convergence is deemed after 30 training epochs.

We randomly selected some images from the MNIST test dataset to evaluate IGMC. The results are presented in Table 1. The black numbers in the table represent the percentage probability of a prediction belonging to the corresponding category. The number in red inside the square brackets is  $4\sigma^2$ , where  $\sigma^2$  is the variance of the  $F_{H,N}$  for the corresponding category returned by IGMC. This red number can be viewed as a measure of uncertainty, ranging from 0.0 to 1.0. A larger value indicates greater uncertainty.

We also test different rotation angles of an image and some letter images from the EMNIST dataset (Cohen et al., 2017) to simulate the situation where the test data are out of distribution. The results are shown in Table 2 and Table 3.

Labels								
0	0.0[0.00]	0.0[0.00]	0.6[0.01]	0.0[0.00]	0.0[0.00]	0.0[0.00]	6.1[0.19]	17.4[0.46]
1	0.0[0.00]	0.1[0.00]	0.0[0.00]	0.0[0.00]	0.1[0.00]	0.0[0.00]	0.0[0.00]	0.0[0.00]
2	0.0[0.00]	11.5[0.33]	77.6[0.57]	0.1[0.00]	12.9[0.28]	0.0[0.00]	3.3[0.11]	1.2[0.03]
3	0.0[0.00]	0.0[0.00]	2.4[0.04]	93.2[0.19]	70.6[0.52]	0.1[0.00]	0.0[0.00]	0.1[0.00]
4	100.0[0.00]	78.8[0.54]	3.4[0.10]	0.0[0.00]	0.0[0.00]	27.2[0.63]	35.2[0.71]	19.6[0.50]
5	0.0[0.00]	0.0[0.00]	0.0[0.00]	5.4[0.15]	4.7[0.11]	36.6[0.78]	9.4[0.25]	2.2[0.06]
6	0.0[0.00]	2.8[0.10]	0.9[0.03]	0.0[0.00]	0.1[0.00]	18.4[0.52]	28.3[0.64]	3.2[0.10]
7	0.0[0.00]	0.0[0.00]	7.1[0.20]	1.2[0.03]	10.1[0.22]	3.3[0.10]	11.6[0.35]	55.0[0.78]
8	0.0[0.00]	0.6[0.02]	2.4[0.08]	0.1[0.00]	0.4[0.00]	0.0[0.00]	0.1[0.00]	0.5[0.01]
9	0.0[0.00]	6.2[0.18]	5.6[0.17]	0.0[0.00]	1.2[0.02]	14.3[0.41]	5.9[0.15]	0.8[0.01]

Table 2: Results for different rotations of an image.

Labels								
0	0.0[0.00]	1.5[0.04]	37.8[0.81]	91.8[0.24]	41.0[0.82]	0.0[0.00]	0.5[0.01]	1.4[0.05]
1	0.0[0.00]	3.1[0.09]	0.0[0.00]	0.0[0.00]	0.0[0.00]	21.7[0.54]	0.0[0.00]	0.2[0.00]
2	0.0[0.00]	7.4[0.19]	0.0[0.00]	0.0[0.00]	18.2[0.46]	7.7[0.23]	0.0[0.00]	98.2[0.05]
3	2.1[0.07]	1.7[0.05]	0.0[0.00]	0.0[0.00]	0.1[0.00]	0.0[0.00]	38.4[0.80]	0.2[0.00]
4	0.0[0.00]	0.0[0.00]	56.6[0.85]	6.9[0.20]	32.5[0.73]	1.0[0.03]	37.1[0.83]	0.0[0.00]
5	97.9[0.07]	0.8[0.03]	0.0[0.00]	0.0[0.00]	1.0[0.04]	0.8[0.02]	19.7[0.54]	0.0[0.00]
6	0.0[0.00]	0.0[0.00]	4.4[0.13]	1.3[0.04]	1.0[0.03]	0.0[0.00]	0.0[0.00]	0.1[0.00]
7	0.0[0.00]	13.8[0.34]	0.0[0.00]	0.0[0.00]	0.0[0.00]	0.0[0.00]	3.6[0.10]	0.0[0.00]
8	0.0[0.00]	71.7[0.62]	1.0[0.03]	0.0[0.00]	6.2[0.18]	68.7[0.73]	0.1[0.00]	0.0[0.00]
9	0.0[0.00]	0.1[0.00]	0.1[0.00]	0.0[0.00]	0.1[0.00]	0.0[0.00]	0.6[0.01]	0.0[0.00]

Table 3: Results for images from EMNIST dataset.

## 5 Conclusion and future work

We propose a simple and intuitive method, IGMC, that utilizes generative approaches to compute the posterior distribution of neural network predictions. We provide a convergence rate guarantee for IGMC and validate IGMC using a small convolutional architecture on the MNIST dataset.

IGMC still has many limitations. It needs a good  $\Phi$  as a substitute for the prior and likelihood in the Bayesian method, but verifying whether  $\Phi$  meets the requirements is not straightforward. IGMC requires generating  $N \times H$  times, which can be computationally expensive, especially when evaluating the uncertainty of large neural networks since it involves training the generative model multiple times. We will study how to optimize IGMC in the future.

## References

- Murat Seckin Ayhan and Philipp Berens. Test-time data augmentation for estimation of heteroscedastic aleatoric uncertainty in deep neural networks. In *International conference on Medical Imaging with Deep Learning*, 2018.
- Kamyar Azizzadenesheli, Emma Brunskill, and Animashree Anandkumar. Efficient exploration through bayesian deep q-networks. *CoRR*, abs/1802.04412, 2018.
- Marc G. Bellemare, Sriram Srinivasan, Georg Ostrovski, Tom Schaul, David Saxton, and Rémi Munos. Unifying count-based exploration and intrinsic motivation. In *Proceedings of the 30th International Conference on Neural Information Processing Systems, NIPS' 16*, page 1479–1487, Red Hook, NY, USA, 2016. Curran Associates Inc. ISBN 9781510838819.
- Charles Blundell, Julien Cornebise, Koray Kavukcuoglu, and Daan Wierstra. Weight uncertainty in neural networks. In *Proceedings of the 32nd International Conference on International Conference on Machine Learning - Volume 37, ICML' 15*, page 1613–1622. JMLR.org, 2015.
- Jiwoong Choi, Dayoung Chun, Hyun Kim, and Hyuk-Jae Lee. Gaussian yolov3: An accurate and fast object detector using localization uncertainty for autonomous driving. In *Proceedings of the IEEE/CVF International Conference on Computer Vision (ICCV)*, October 2019.
- Gregory Cohen, Saeed Afshar, Jonathan Tapson, and André van Schaik. Emnist: an extension of mnist to handwritten letters, 2017.
- Li Deng. The mnist database of handwritten digit images for machine learning research. *IEEE Signal Processing Magazine*, 29(6):141–142, 2012.
- Di Feng, Lars Rosenbaum, and Klaus Dietmayer. Towards safe autonomous driving: Capture uncertainty in the deep neural network for lidar 3d vehicle detection. In *2018 21st International Conference on Intelligent Transportation Systems (ITSC)*, pages 3266–3273, 2018.
- Yarin Gal and Zoubin Ghahramani. Dropout as a bayesian approximation: Representing model uncertainty in deep learning. *Proceedings of The 33rd International Conference on Machine Learning*, 06 2015.
- Yarin Gal, Riashat Islam, and Zoubin Ghahramani. Deep bayesian active learning with image data. 03 2017.
- Ian J. Goodfellow, Jean Pouget-Abadie, Mehdi Mirza, Bing Xu, David Warde-Farley, Sherjil Ozair, Aaron Courville, and Yoshua Bengio. Generative adversarial networks, 2014.
- Dan Hendrycks and Kevin Gimpel. A baseline for detecting misclassified and out-of-distribution examples in neural networks. 10 2016.
- Jonathan Ho, Ajay Jain, and Pieter Abbeel. Denoising diffusion probabilistic models. *arXiv preprint arxiv:2006.11239*, 2020.
- Eyke Hüllermeier and Willem Waegeman. Aleatoric and epistemic uncertainty in machine learning: an introduction to concepts and methods. *Machine Learning*, 110, 03 2021.
- Lie Ju, Xin Wang, Lin Wang, Dwarikanath Mahapatra, Xin Zhao, Quan Zhou, Tongliang Liu, and Zongyuan Ge. Improving medical images classification with label noise using dual-uncertainty estimation. *IEEE Transactions on Medical Imaging*, PP:1–1, 01 2022.
- Diederik P Kingma and Max Welling. Auto-encoding variational bayes, 2022.
- Balaji Lakshminarayanan, Alexander Pritzel, and Charles Blundell. Simple and scalable predictive uncertainty estimation using deep ensembles. In *Proceedings of the 31st International Conference on Neural Information Processing Systems, NIPS' 17*, page 6405–6416, Red Hook, NY, USA, 2017. Curran Associates Inc. ISBN 9781510860964.
- Yann LeCun, Y. Bengio, and Geoffrey Hinton. Deep learning. *Nature*, 521:436–44, 05 2015.

- Kimin Lee, Honglak Lee, Kibok Lee, and Jinwoo Shin. Training confidence-calibrated classifiers for detecting out-of-distribution samples. 11 2017.
- Subhabrata (Subho) Mukherjee and Ahmed H. Awadallah. Uncertainty-aware self-training for few-shot text classification. In *NeurIPS 2020 (Spotlight)*. ACM, December 2020.
- Tanya Nair, Doina Precup, Douglas L. Arnold, and Tal Arbel. Exploring uncertainty measures in deep networks for multiple sclerosis lesion detection and segmentation. *Medical Image Analysis*, 59:101557, 2020. ISSN 1361-8415.
- Philipp Oberdiek, Matthias Rottmann, and Hanno Gottschalk. Classification uncertainty of deep neural networks based on gradient information. In Luca Pancioni, Friedhelm Schwenker, and Edmondo Trentin, editors, *Artificial Neural Networks in Pattern Recognition*, pages 113–125, Cham, 2018. Springer International Publishing. ISBN 978-3-319-99978-4.
- Abhijit Guha Roy, Sailesh Conjeti, Nassir Navab, and Christian Wachinger. Bayesian quicknat: Model uncertainty in deep whole-brain segmentation for structure-wise quality control. *NeuroImage*, 195: 11–22, 2019. ISSN 1053-8119.
- Philipp Seeböck, José Orlando, Thomas Schlegl, Sebastian Waldstein, Hrvoje Bogunović, Sophie Riedl, Georg Langs, and Ursula Schmidt-Erfurth. Exploiting epistemic uncertainty of anatomy segmentation for anomaly detection in retinal oct. *IEEE Transactions on Medical Imaging*, PP: 1–1, 05 2019.
- Murat Sensoy, Lance Kaplan, and Melih Kandemir. Evidential deep learning to quantify classification uncertainty. In *Proceedings of the 32nd International Conference on Neural Information Processing Systems*, NIPS’18, page 3183–3193, Red Hook, NY, USA, 2018. Curran Associates Inc.
- Dominik Seuß. Bridging the gap between explainable ai and uncertainty quantification to enhance trustability. 05 2021.
- Artem Shelmanov, Dmitri Puzyrev, Lyubov Kupriyanova, Denis Belyakov, Daniil Larionov, Nikita Khromov, Olga Kozlova, Ekaterina Artemova, Dmitry V. Dylov, and Alexander Panchenko. Active learning for sequence tagging with deep pre-trained models and Bayesian uncertainty estimates. In *Proceedings of the 16th Conference of the European Chapter of the Association for Computational Linguistics: Main Volume*, pages 1698–1712, Online, April 2021. Association for Computational Linguistics.
- Matias Valdenegro-Toro. Deep sub-ensembles for fast uncertainty estimation in image classification. *arXiv preprint arXiv:1910.08168*, 2019.
- Guotai Wang, Wenqi Li, Michael Aertsen, Jan Deprest, Sébastien Ourselin, and Tom Vercauteren. Aleatoric uncertainty estimation with test-time augmentation for medical image segmentation with convolutional neural networks. *Neurocomputing*, 338:34–45, 2019. ISSN 0925-2312.
- Zhizheng Zhang, Cuiling Lan, Wenjun Zeng, Zhibo Chen, and Shih-Fu Chang. Uncertainty-aware few-shot image classification. In *International Joint Conference on Artificial Intelligence (IJCAI 2021)*, June 2021.

## A Proof of Theorem 1

Considering that  $\hat{F}_{H,N}$  is the empirical distribution obtained by sampling  $N$  observations followed by the distribution function  $F_H$ , our proof can be divided into the following two parts:

### A.1 Distance between $F_H$ and $F_\infty$

Let  $\{y_k\}$  be a sequence of random variables satisfying  $y_k \sim \Phi(\mathcal{S}, y_1, \dots, y_{k-1})$ , where  $\mathcal{S} = x_1, \dots, x_M$ . Let  $Z_K = \frac{\sum x + \sum y_k}{M+K}$ , and  $\mu = Z_H$ .

Since  $X$  in range  $[0, 1]$ , we have  $E[|Z_K|] \leq 1$ . And because there is  $E[\Phi(\mathcal{S}')] = \text{mean}(\mathcal{S}')$  for any set  $\mathcal{S}'$ , obviously  $\{Z_k\}$  is a martingale with respect to the filtration  $\mathcal{F}_k = \sigma(y_1, \dots, y_k)$ , and the differences of  $\{Z_k\}$  satisfies

$$|Z_k - Z_{k-1}| = \frac{1}{k+M} |Z_{k-1} + y_k| \leq \frac{2}{k+M}$$

According to the Azuma-Hoeffding inequality, following inequality holds for any  $K > H$ :

$$\Pr(|Z_K - \mu| \geq a) \leq 2 \exp \left( - \frac{2a^2}{\sum_{k=H+1}^K \left( \frac{2}{k+M} \right)^2} \right)$$

When  $K \rightarrow \infty$ , we have

$$\lim_{K \rightarrow \infty} \Pr(|Z_K - \mu| \geq a) \leq 2 \exp \left( - \frac{H+M}{2} a^2 \right)$$

We sample  $\{y_k\}$  sequence for  $S$  times, let  $\{y_k^s\}$  be the sequence observed in the  $s$ -th sampling and  $Z_K^s = \frac{\sum x + \sum y_k^s}{M+K}$ . Then

$$\hat{F}_{K,S}^\Phi(t) = \frac{1}{S} \sum_{s=1}^S \mathbb{I}(Z_K^s < t)$$

is the empirical distribution by sampling  $S$  times from  $F_K$ .

By the Glivenko–Cantelli theorem, when  $S \rightarrow \infty$ ,  $\sup_t |\hat{F}_{K,S}(t) - F_K(t)| \xrightarrow{a.s.} 0$ , so

$$\begin{aligned} \|F_H(t) - F_\infty(t)\|_1 &= \int_0^1 |F_H(t) - F_\infty(t)| dt \\ &= \int_0^1 \left| F_H(t) - \lim_{K \rightarrow \infty} F_K(t) \right| dt \\ &= \int_0^1 \left| \lim_{S \rightarrow \infty} \left( \hat{F}_{H,S}(t) - \lim_{K \rightarrow \infty} \hat{F}_{K,S}(t) \right) \right| dt \\ &= \int_0^1 \left| \lim_{S \rightarrow \infty} \frac{1}{S} \sum_{s=1}^S \left( \mathbb{I}(Z_H^s < t) - \lim_{K \rightarrow \infty} \mathbb{I}(Z_K^s < t) \right) \right| dt \\ &\leq \lim_{S \rightarrow \infty} \frac{1}{S} \sum_{s=1}^S \int_0^1 \left| \mathbb{I}(Z_H^s < t) - \lim_{K \rightarrow \infty} \mathbb{I}(Z_K^s < t) \right| dt \\ &= \lim_{S \rightarrow \infty} \frac{1}{S} \sum_{s=1}^S \left| \lim_{K \rightarrow \infty} Z_K^s - Z_H^s \right| \end{aligned}$$

$$\begin{aligned}
&= \mathbb{E} \left[ \lim_{K \rightarrow \infty} |Z_K - Z_H| \right] \\
&= \int_0^1 \lim_{K \rightarrow \infty} \Pr(|Z_K - Z_H| > a) da \\
&\leq \int_0^1 2 \exp\left(-\frac{M+H}{2} a^2\right) da \\
&< \sqrt{\frac{2\pi}{M+H}}
\end{aligned}$$

## A.2 Distance between $\hat{F}_{H,N}$ and $F_H$

By Dvoretzky–Kiefer–Wolfowitz inequality, we have

$$\Pr \left( \sup_{x \in [0,1]} \left( \hat{F}_{H,N}^\Phi(t) - F_H^\Phi(t) \right) > a \right) \leq 2 \exp(-2Na^2) \quad (8)$$

Subsequently

$$\begin{aligned}
\mathbb{E} \left[ \left\| \hat{F}_{H,N}^\Phi(t) - F_H^\Phi(t) \right\|_1 \right] &= \int_0^1 a \cdot \Pr \left( \left\| \hat{F}_{H,N}^\Phi(t) - F_H^\Phi(t) \right\|_1 = a \right) da \\
&= \int_0^1 \Pr \left( \left\| \hat{F}_{H,N}^\Phi(t) - F_H^\Phi(t) \right\|_1 \geq a \right) da \\
&\leq \int_0^1 \Pr \left( \sup_{t \in [0,1]} \left( \hat{F}_{H,N}^\Phi(t) - F_H^\Phi(t) \right) \geq a \right) da \\
&\leq \int_0^1 2 \exp(-2Na^2) da \\
&< \sqrt{\frac{\pi}{2N}}
\end{aligned}$$

We complete the proof by combining the results of A.1 and A.2. □